Research Article

Cancer Prevention Research

Fiberoptic Resonance Raman Spectroscopy to Measure Carotenoid Oxidative Breakdown in Live Tissues

Brandon G. Bentz[1,3], Jason Diaz[5], Terry A. Ring[4], Mark Wade[2], Konrad Kennington[1], David M. Burnett[1], Robert McClane[1], and Frank A. Fitzpatrick[6]

Abstract

Based on compelling epidemiologic and corroboratory *in vitro* studies, carotenoids are thought to have great potential as dietary prevention against cancer. Yet, carotenoid-based chemopreventive trials have found very contradictory results. Definitive conclusions from these trials are hampered by an inability to accurately and safely measure carotenoids in specific tissues at risk of cancer development. Raman spectroscopy has been proposed as an optical technology with which to analyze various molecules in live tissues. One major obstacle that impedes the clinical use of this powerful technology is the lack of a fiberoptic Raman probe suitable for endoscopic tissue evaluation. A single-fiber resonance Raman Spectroscope capable of noninvasive "optical biopsies" to measure carotenoid concentrations in live tissues has been developed. The accuracy of this Raman instrument was confirmed by comparison with more standard methods of spectrophotometry and high-pressure liquid chromatography using solubilized β-carotene (BC) and BC-loaded cells before use in a small patient cohort. This Raman instrument detected intact BC as well as BC oxidative breakdown as a decrement of its Raman signal in cells. Use of the Raman instrument in our small cohort study showed its feasibility for measuring human tissues and raised some potentially intriguing possibilities about BC tissue pharmacokinetics and oxidative biology. Based on these results, our newly developed single fiberoptic resonance Raman instrument may provide a very useful method of measuring carotenoids and their oxidative breakdown within live tissue during future carotenoid chemopreventive trials. This proof-of-concept study provides the foundation to justify future validation of our Raman prototype. *Cancer Prev Res; 3(4); 529–38. ©2010 AACR.*

Introduction

Tobacco smoking is a major global health concern, causing an estimated 100 million deaths during the 20th and an anticipated 1 billion deaths in the 21st century (1). Cancer is the second leading causes of death attributable to smoking (2), with an estimated 15 million new cancer cases diagnosed annually worldwide by 2020 leading to an annual death toll of more than 12 million people (3). Two of the most important modifiable risk factors for the development of cancers are tobacco use and diets high in saturated fats and deficient in fruits, vegetables, and whole grains (1). Thus, research focusing on the relationship between tobacco, diet, and cancer has the potential to significantly improve global health.

Numerous epidemiologic studies have consistently shown that diets high in fruits, vegetables, and whole grains are associated with a reduced risk of developing such chronic diseases as cardiovascular disease and cancer through what is thought to be a reduction in oxidative stress (4–6). Therefore, dietary-based cancer interventions seem to be practical targets for potentially reducing the risk of cancer development. Phytochemicals are bioactive nonnutrient plant compounds found in fruits, vegetables, and whole grains that are thought to have great potential as chemopreventive agents. One of the most widely studied subclasses of phytochemicals is the carotenoids (7). Carotenoids are fat-soluble pigments composed predominantly by an all-*trans* polyene-conjugated double-bond backbone of eight isoprenoid units. This conjugated polycarbon backbone is efficient at trapping singlet oxygen or nitrogen radicals, thus reducing oxidative stress (8) and therefore

Authors' Affiliations: [1]Division of Otolaryngology-Head and Neck Surgery, Department of Surgery and [2]Department of Oncologic Sciences, The Huntsman Cancer Institute, University of Utah School of Medicine; [3]George E. Wahlen Veterans Administration Hospital; [4]Department of Chemical Engineering, University of Utah, Salt Lake City, Utah; [5]Department of Otolaryngology-Head and Neck Surgery, Washington University School of Medicine, St. Louis, Missouri; and [6]Department of Pharmacology, Kansas City University of Medicine and Biosciences, Kansas City, Missouri

Corresponding Author: Brandon G. Bentz, Division of Otolaryngology-Head and Neck Surgery, Department of Surgery, University of Utah School of Medicine, 3C120 SOM, 50 North Medical Drive, Salt Lake City, UT 84132. Phone: 801-581-7515, Fax: 801-585-5744; E-mail: brandon.bentz@hci.utah.edu.

doi: 10.1158/1940-6207.CAPR-09-0157

potentially reducing the risk of cancer. In addition, carotenoids seem to offer a variety of other mechanisms of cancer protection (8), contributing to their overall cancer benefit. Based on prevailing epidemiologic and *in vitro* data, clinical trials have explored the use of carotenoids as cancer chemopreventive agents.

Despite scientific optimism that specific phytochemicals such as carotenoids may represent the "magic bullet" to cancer prevention, the true effect of carotenoids on the incidence of cancer has been brought into question as clinical trial results have suggested that carotenoid supplementation may confer no benefit or may actually increase the risk of tobacco-related cancer development in subjects who are actively or formerly smoking (9–12). A better understanding of the nuances of carotenoid biology may allow for tailoring of chemopreventive interventions based on the modes of action of carotenoid under various oxidative conditions.

One obvious pitfall of these chemopreventive trials that makes definitive conclusions impossible is a lack of an ability to measure carotenoid pharmacokinetics within the specific tissues at risk of cancer development. Previous chemopreventive trials have estimated carotenoid bioavailability by measuring dietary intake or serum concentrations. Estimations of carotenoid bioavailability by these methods are fraught with many shortcomings (13). Because carotenoids are hydrophobic and predominantly associated with lipid domains of foods and tissues, lipid-containing foods that are ingested with the carotenoid source can significantly affect absorption. The measurement of serum concentrations must take into account several dynamic processes including gut absorption, chylomicron response, conversion to other interrelated carotenoids, isomerization, and tissue absorption. Present studies evaluating carotenoid intake or serum concentrations are only very rough estimates of carotenoid bioavailability and pharmacokinetics in at-risk tissues. Therefore, methods to measure carotenoid concentrations within specific tissues have great potential for further defining carotenoid biopharmacology.

Raman spectroscopy is a particularly powerful analytic technique that offers great promise for its ability to quantify specific molecular species in complex matrices, such as human tissues. When monochromatic light illuminates a chemical compound, a minute fraction of the incident light can be scattered inelastically, with one or more discrete shifts in wavelength. These light wavelength shifts, termed Stokes shifts, corresponds exactly to the various vibrational energy levels of the light scattering molecules. This process, termed Raman scattering, can provide a highly specific optical fingerprint of the molecules of interest (14, 15). Raman scattering intensity is proportional to the concentration of the scattering molecules. Ordinarily, Raman spectroscopy in biological systems yields a complex spectrum of light from the wide variety of chemical compounds present. Moreover, these spectral peaks tend to be of weak intensity due to only a small proportion of the scattered light being Raman shifted. Under specific circumstances, when the incident light overlaps the optical absorption band of a molecule, the Raman signal can be resonantly enhanced by many orders of magnitude. Carotenoids have particularly intense absorption bands in the blue/green wavelength range that result in a large (~5 orders of magnitude) resonant enhancement of the Raman signal. No other Raman-active biological molecules found in significant concentrations in human tissues exhibit similar Raman shifts and resonant enhancement within the carotenoid absorption bands. Therefore, in live tissues, resonance-enhanced Raman carotenoid spectra are selectively enhanced by several orders of magnitude above confounding background signals to potentially produce a remarkably high-contrast Raman measurement.

One major obstacle hindering the use of Raman spectroscopy in a clinical setting has been the lack of a fiberoptic probe easily adaptable to a variety of clinical settings. Herein, we report the construction and initial clinical evaluation of a single-fiber fiberoptic instrument

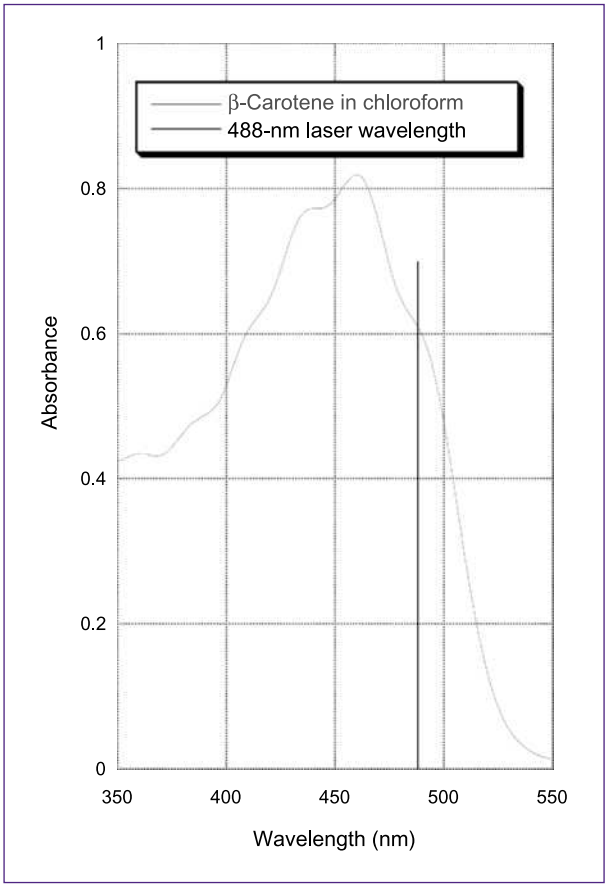

Fig. 1. Absorption spectrum for β-carotene. Visible light was used to determine an absorption spectrum for BC. BC was solubilized in chloroform, and the absorbance was determined between 350 and 550 nm of incident light. Based on this absorption spectrum, we chose an incident resonance wavelength of 488 nm (delimited by the black line).

suitable for resonance-enhanced Raman measurements of carotenoid in any live tissues endoscopically accessible. Our results show the feasibility of our fiberoptic Raman instrument to measure carotenoid concentrations instantaneously and noninvasively. These data support further validation of this new technology, which could potentially dramatically improve future carotenoid-based clinical trials.

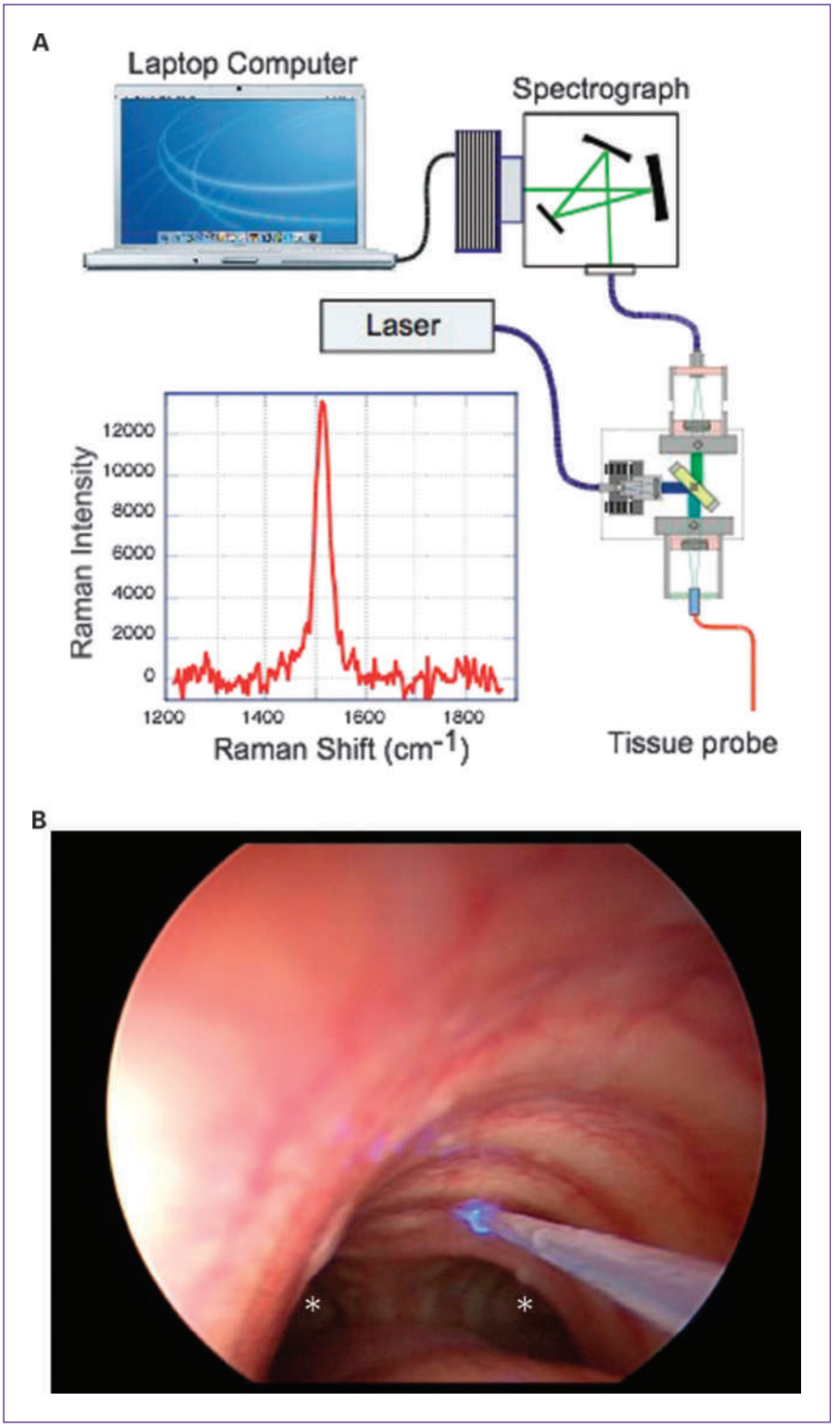

Fig. 2. Single-fiber resonance-enhanced Raman spectroscope. A, light from an argon laser is routed into an optical module where a specially designed holographic optical element couples the laser light (~1 mW) into an endoscope-compatible single optical fiber probe. The probe is momentarily (~12 s) held in contact with tissue during a measurement. Laser light illuminates the tissue, and back-scattered light is collected by the probe and routed back to the optical module where the holographic optical element selectively accepts the Raman-shifted wavelength of light and routes this light into another fiber optic cable connected to a compact high-throughput spectrograph equipped with a high dynamic range charge-coupled device detector interfaced with a laptop computer running software designed specifically for making quantitative *in vivo* Raman measurements. The isolated 1,525 cm^{-1} carotenoid peak from a volunteer's soft palate is characterized using a Lorentzian line shape and has been found to be linearly proportional to the tissue carotenoid concentrations in live tissue (14, 15). B, Fiberoptic probe measuring tracheal mucosa shows the ready use for measuring any tissue that is endoscopically accessible. A 600-μm fiberoptic probe was inserted through a ventilating bronchoscope. The probe was brought into contact with the tracheal mucosa just superior to the carina and mainstem bronchi (*). The mucosa was illuminated with the blue/green laser light and Raman measurements were made through the same fiberoptic probe.

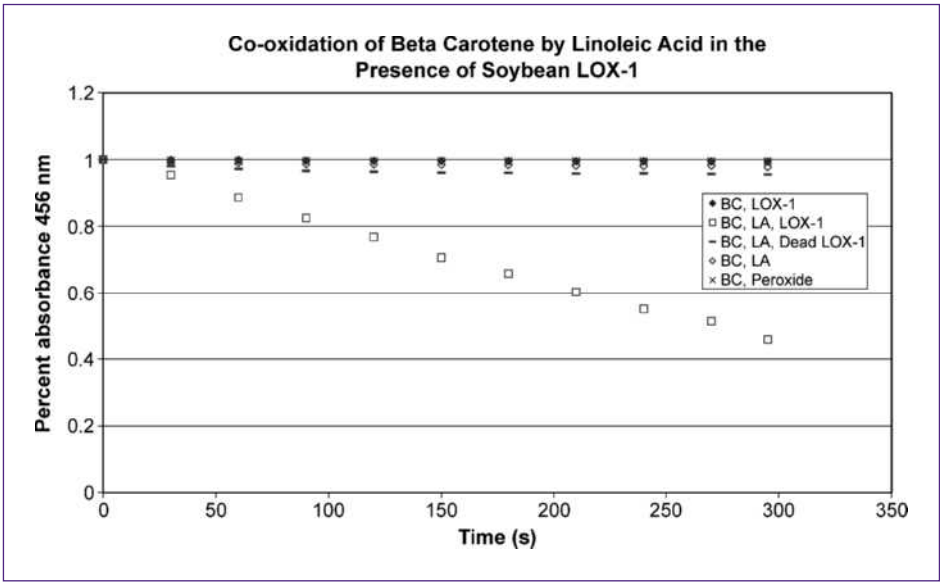

Fig. 3. Co-oxidation of BC in the presence of LOX-1/linoleic acid. Solubilized BC (1 mmol/L) was incubated in the presence of soybean lipoxygenase (LOX)-1 and linoleic acid (LA) either separately or together and photobleaching was measured as the percent absorbance at 456 nm. Control exposure to inactive LOX-1 (Dead LOX-1) was used to confirm LOX specific activity. The co-oxidation of BC in the presence of another oxidative stress, peroxide, was also measured for comparison. As seen, a decrease in percent absorbance was noted only in the presence of LOX-1/linoleic acid together, but not with either LOX-1 or linoleic acid alone or in the presence of dead LOX-1/linoleic acid. Peroxide was used as an alternate source of oxidative stress for comparison with the generation of endogenous oxidative stress by LOX. No appreciable decrement in absorbance was noted for 1 mol/L peroxide. These data confirm and expand on prior published data that show co-oxidation of BC under these conditions (25).

Materials and Methods

Single-fiber resonance-enhanced Raman spectroscope

We have designed a Raman instrument able to use a single optical fiber compatible with standard endoscopes. Based on the absorption spectrum of β-carotene (BC; Fig. 1), an excitation laser (Spectra-Physics model 163) at 488 nm was chosen for this prototype. As shown in Fig. 2, the laser light is launched into a multimode optical fiber patch cable (SMA-connectorized 300-μm polymer-clad silica fiber; 3M). This excitation fiber is then connected to a custom-made optical module via a collimator and gimbal mount. The collimated laser light is directed into a custom-made holographic optical element (Ralcon Development Lab) at an angle such that it is diffracted toward a lens focusing the light into a SMA-connectorized endoscopy probe fiber (200- to 600-μm polymer-clad silica fiber, 0.22-0.48 numerical aperture, with Tefzel jacket) that is flat-cut and polished flush with the jacket to make it compatible with most endoscope channels. The probe fiber serves both as an excitation fiber and as a scattered light collection fiber, directing the back-scattered light toward the optical module where it is collimated and passed through the holographic optical element. The considerable Rayleigh scattered light (light that has not been wavelength shifted via the Raman effect) from the tissue is diffracted out of the collimated beam by the holographic optical element, whereas the Raman-shifted light (and tissue fluorescence, etc.) is selectively passed through the holographic optical element to another lens, which then focuses this signal beam into a SMA-connectorized round-to-linear fiber bundle coupled to the high-throughput compact spectrograph (Spectra-Physics model 77400, with fiber bundle input accessory). A high dynamic range charge-coupled device camera (SBIG ST-9XEI) is used in the spectrograph. The system is connected to a laptop computer running LabView software, which controls the optical system and provides data acquisition and signal analysis. The optical module also contains a software-controlled shutter and laser light intensity monitor, which is used for signal correction.

The probe fiber is 4 m long and can be easily positioned in contact with tissue anywhere there is endoscopic access (see Fig. 2). The probe is momentarily (~5-20 s) held in contact with the tissue under study during a measurement. Laser light illuminates the tissue, and back-scattered light is collected by the probe and routed back to the optical module and then to the spectrograph.

Light entering the spectrograph is a mixture of background signal (broad-band tissue fluorescence, probe fluorescence along with any Raman signals from the probe and module optical components, residual Rayleigh scattered excitation light) and the carotenoid characteristic Raman signal, the carbon double-bond "fingerprint signature" at 1,525 cm^{-1}. Because the BC signal at 1,525 cm^{-1} is the peak of interest, the instrument is designed to specifically collect resonant Raman signals only from the 1,200-1,900 wave number region and block other interfering signals. The software characterizes the relatively intense broad-band background fluorescence within this region

using a polynomial fit and subtracts this component from the composite spectrum, leaving only narrow-band Raman signals for further analysis (Fig. 2). Confounding Raman signals arising from the probe fiber usually preclude using a single fiber for Raman endoscopy in this wave number range (16–18), but in our case, these obstructing signals are out of resonance and/or out of the analysis window and thus cause no interference. The isolated 1,525 cm^{-1} C=C resonance Raman carotenoid peak is further characterized using a Lorentzian line shape, and the peak attributes are reported. The Lorentzian peak height at 1,525 cm^{-1} is proportional to the tissue carotenoid concentration (15, 19). The instrument was calibrated for Stokes shift wave number and intensity using a polycaprolactone polymer standard before measurements are made. In this configuration and with this calibration procedure, this instrument gives relative SDs of less than 10% on all tissue samples. Details of the theoretical basis underlying our initial Resonance-enhanced Raman instruments may be found in previously published studies (20–22).

BC detection before and after oxidation *in vitro*

Confirmation of the ability of this Raman instrument to detect BC before and after oxidative stress in this study was confirmed by comparison to spectrophotometry and high-pressure liquid chromatography (HPLC) measurements.

Based on prior published results (23) showing co-oxidation of BC by soybean lipoxygenase, the ability of 15-lipoxygenase-1 (15-LOX-1), a dioxygenase enzyme that imposes oxidative stress in the presence of arachidonic acid or linoleic acid (24), to induce co-oxidation of BC was first confirmed in solution. For our cell line work, we used ERC293 cells engineered to conditionally express stable *15-LOX-1*. Additionally, ERC293 cells have been engineered to express the corresponding point mutations of these *LOX* genes, which are catalytically inactive as controls. ERC293 cells were maintained in DMEM supplemented with 10% fetal bovine serum, 2 mmol/L L-glutamine, 1 mmol/L sodium pyruvate, nonessential amino acids, and 50 units/mL penicillin and streptomycin (GIBCO/Invitrogen) in a humidified incubator at 37°C with 5% CO_2. Ponasterone A (A.G. Scientific, Inc.), BC (Sigma-Aldrich), linoleic acid (Cayman Chemical), arachidonic acid (Nu-Chek Prep, Inc.), methyl-β-cyclodextrin (MβCD), and soybean lipoxygenase-1 type 1B (15-LOX-1; Sigma-Aldrich) were all used as specified in the following text.

15-LOX-1–engineered ERC293 cells were grown to 80% confluence in media with or without 10 μmol/L ponasterone A as previously described (25). These cells were then exposed overnight to 0.3% (max) methyl-β-cyclodextrin (MβCD) alone or in combination with 0.2 or 1.0 μmol/L BC (26). Cells were incubated for 10 min at 37°C with vehicle or 60 μmol/L arachidonic acid to generate 15-hydroperoxy-5,8,11-*cis*-13-*trans*-eicosatetraenoic acid and oxidant stress (24). At the times indicated, cells were harvested by scraping, washed twice, resuspended in cold PBS, and pelleted by centrifugation (400 × *g*, 5 min). Three sequential Raman measurements of the cell pellet

Table 1. Raman measurements of BC in ERC293 cells

	Treatment groups			Measurements	
	β-Carotene	Arachidonic acid	Ponasterone	Spectrophotometry reading (456 nm)	Raman spectrometry reading
ERC293 cells loaded with β-carotene					
MβCD alone				0.006 ± 0.001	ND
MβCD + 0.2 μmol/L BC				0.0265 ± 0.004*	4,840 ± 43†
MβCD + 1 μmol/L BC				0.04 ± 0.001*	18,995 ± 123†
β-Carotene–loaded ERC293 cells after oxidative stress					
MβCD + 0.2 μmol/L BC	–	–	–		ND
	–	+	–		ND
	–	–	+		ND
	–	+	+		ND
	+	–	–		8,188 ± 243
	+	+	–		8,429 ± 225
	+	–	+		8,730 ± 450
	+	+	+		6,914 ± 48‡

NOTE: ND, signal not detectable over background. Values are expressed as mean ± SEM.

*$P < 0.001$ by Student's *t* test.

†$P = 0.05$ by one-way ANOVA.

‡Significant difference between BC + arachidonic acid + ponasterone vs BC alone ($P < 0.002$), vs BC + arachidonic acid ($P < 0.006$), and vs BC + ponasterone ($P < 0.02$) by ANOVA.

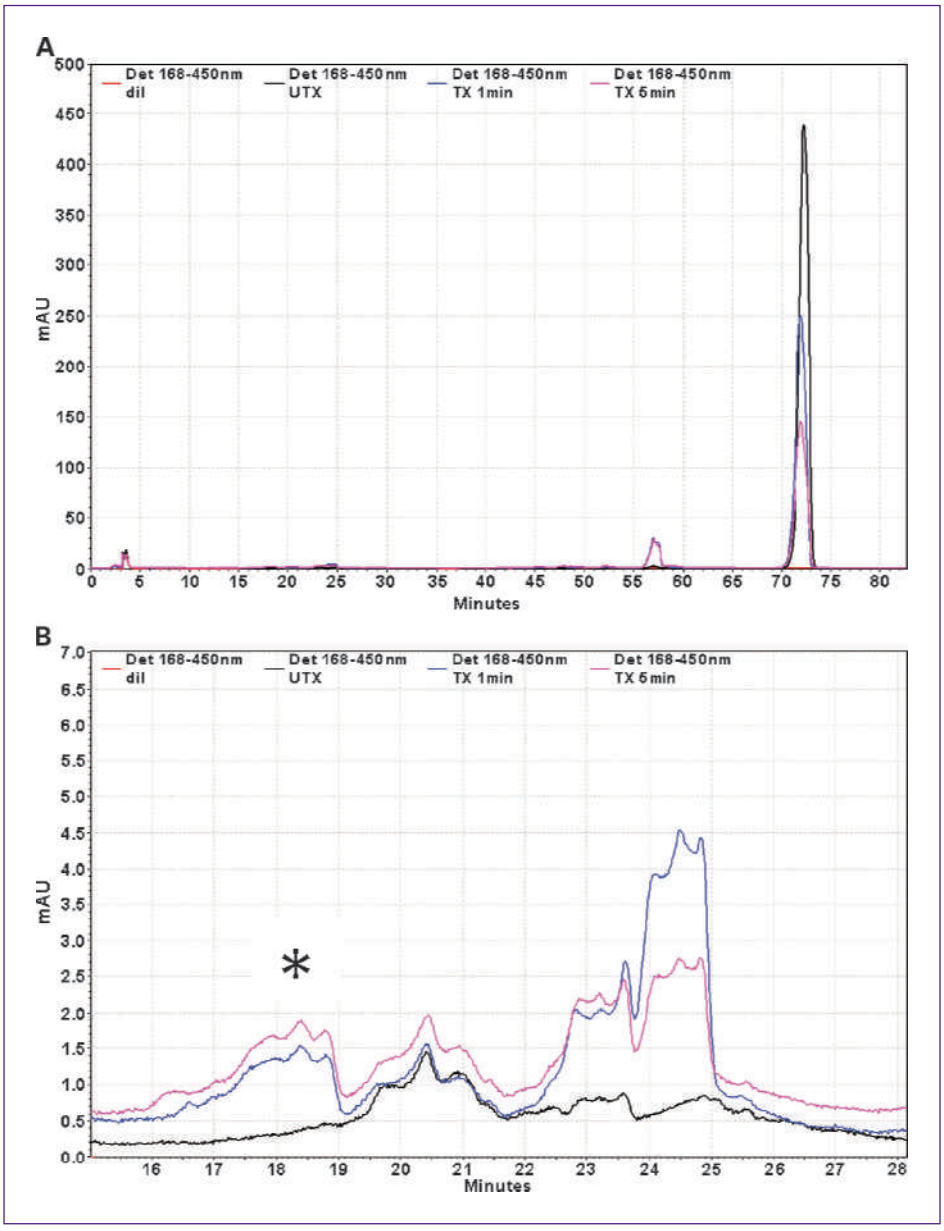

Fig. 4. The appearance over time of β-carotene breakdown products in the presence of LOX/linoleic acid. A, BC was exposed to the same reaction mixture as in Fig. 2 for 24 h. Reactions were extracted three times with an equal volume of diethylether and 0.5 g sodium sulfate to remove all traces of water. The ether fraction was decanted, dried under N_2, and resuspended in acetonitrile/chloroform (3:2) and injected onto HPLC for analysis. Two hundred microliters of the oxidized compound were injected onto a Phenomenex Gemini reversed phase C18 column (250 × 4.6 mm). Compounds were eluted from the column using a gradient method run at 1 mL/min: 0 to 5 min methanol/H_2O (9:1); 5 to 20 min MeCN (100%); 20 to 35 min MeCN/ethyl acetate (85:15); 35 to 85 min MeCN/ethyl acetate (85:15); returned to methanol/H_2O over 5 min; then equilibrated for 30 min. Using a Beckman System Gold HPLC with Photodiode Array detector, compounds were detected by measuring the absorbance from 250 to 500 nm. A, using the Beckman 32 Karat Software, we were able to visualize the absorbance spectra and determine the λ_{max} for each compound. As seen, diluent alone (red line) showed no detectable peak, whereas the parent BC peak (t_R = 71 min and a λ_{max} = 450 nm) decreased over time from t = 0 min (black line) through t = 1 min (blue line) to t = 5 min (fuschia line). B, alternative peaks with lower retention times appeared over the same time frame.

were obtained and averaged. The cell pellet was subsequently solubilized following the method of Chichili et al. (27), and BC was extracted with ethanol/hexane and quantified by absorption spectrophotometry at 456 nm. Results were correlated with Raman measurements of BC in pelleted cells.

BC was also extracted from our cell pellets for HPLC by freeze/thawing the pellet in liquid nitrogen, solubilizing with ethanol, and extracting BC with three hexane extractions. Hexane was evaporated over nitrogen in a Rotovap. These samples were fractionated by HPLC on a Phenomenex Gemini C18 analytic column eluted with mobile phase consisting of 65:25:10 (v/v/v) acetonitrile/methylene chloride/methanol with 1 g/L butylated hydroxytoluene and 100 μL/L diisoproplyethylamine at 1 mL/min. For each experimental run, BC standard was used to determine the retention time for unoxidized BC. One hundred microliters of our standard or cell sample were injected onto the column and compounds were separated by monitoring the absorbance of the column effluent at a wavelength of ≈450 nm. These experiments determined if an increase in Raman signal detectable after loading was attributable to BC. Moreover, we used HPLC to determine if a decrement in Raman signal after oxidative stress correlated with a decrease in the spectrophotometric signal and HPLC peak area.

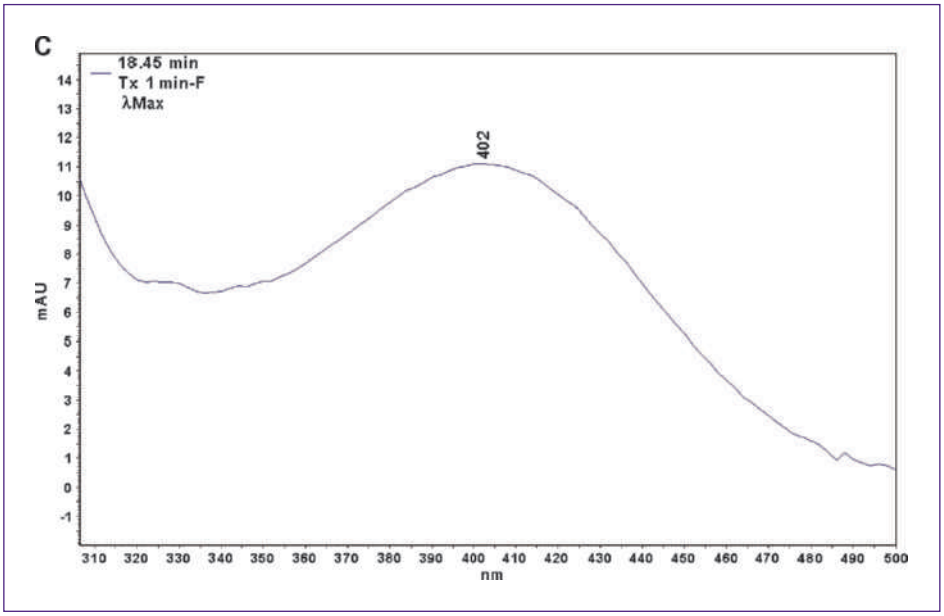

Fig. 4. ***Continued.*** C, one candidate peak was chosen (* in B) and found to have a t_R = 18.45 min and a λ_{max} = 402 nm similar to 5,6-epoxy-β-apo-12′- or -10′-carotenal (23).

Resonance-enhanced Raman spectroscopy in a patient feasibility study

Human subject studies were approved by the Institutional Review Board of the University of Utah. Each participant was given a short validated clinical questionnaire, the AUDIT questionnaire, with supplemental dietary questions (28). Despite the low power (<2 mW, comparable to a laser pointer) and the high divergence of laser light emitted from the fiber, directing the Raman fiber into any subject's eye was avoided.

The feasibility of the single-fiber endoscopic Raman measurements was evaluated by using the Raman instrument in a volunteer undergoing routine bronchoscopic evaluation of the lower respiratory system during clinical treatment. We also determined the feasibility of Raman measurements in a cohort of patients. Using Raman spectroscopy, carotenoid levels were measured at four subsites of the upper aerodigestive tract (UADT; the buccal mucosa, anterior floor of mouth, oral tongue, and soft palate) by the techniques of Hata et al. (15). Answers to these questions were correlated with Raman-measured UADT carotenoid concentrations. The Raman fiberoptic probe was brought into contact with each subsite three times for the requisite exposure time (~12 s) necessary to obtain a characteristic waveform at 1,525 cm^{-1} wavelength, and the peak amplitude was recorded. To control for variations in the optical properties of regions within a subsite, three independent measures within a given subsite of the UADT were measured and the average of three measurements was reported. Variations in the optical properties within a subsite were minimized by consistently identifying the following anatomic landmarks with which to make measurements (1 cm right of the midline raphe of the tip of the oral tongue, 1 cm posterior to the right vermilion commissure on the buccal mucosa, 1 cm posterior of the right Wharton's duct on the floor of mouth, and 1 cm right of midline just posterior to the junction of the hard and soft palate). These mucosal sites were visually inspected for any gross pathologic processes that may affect the Raman measurements (i.e., tumor or inflammatory processes). If these areas were noted to have gross mucosal changes, the subject was eliminated from the study.

Statistical analysis

Statistical analysis of the relationship of categorical clinical variables to Raman measurements was undertaken by a dedicated biostatistician. *P* values were determined using Statistica 6.0 statistical analysis package (StatSoft, Inc.) and a two-sided Fisher's exact test was used for comparison of binary variables and a Pearson χ^2 test was used for variables with three or more categories. Categorical variables with two categories tested for a continuous dependent variable output were analyzed by a Student's *t* test, whereas more than two categorical variables for a continuous dependent variable output were tested using an ANOVA test. If the data were not normally distributed, log transformation was undertaken and statistical significance was established at $P < 0.05$, and values were expressed ±SEM.

Results

Detecting β-carotene in loaded ERC293 cells

Using prior published results (23) showing the co-oxidation of BC in the presence of linoleic acid and soybean lipoxygenase-1, we confirmed that we could show a

Table 2. Use of Raman spectroscopy in patient feasibility study

Categories of analysis			Raman reading	Significance
UADT subsites	Anterior tongue (n = 52)		3,325 ± 255	
	Buccal mucosa (n = 52)		6,944 ± 565	
	Floor of mouth (n = 52)		7,756 ± 684	
	Soft palate (n = 52)		8,620 ± 716	$P < 0.001$*
Alcohol consumption	Floor of mouth	Former/present (n = 27)	11,210 ± 1,319	
		Never (n = 25)	6,994 ± 798	$P < 0.05$
	Soft palate	Former/present (n = 27)	11,269 ± 1,181	
		Never (n = 25)	7,871 ± 892	$P < 0.05$
HNSCCa	Soft palate	Case (n = 6)	3.82 ± 0.13†	
		Control (n = 6)	4.06 ± 0.08†	$P = 0.002$

*Comparison of anterior tongue to other subsites.
†Log-transformed data for case/control comparison.

co-oxidation of BC with *15-LOX-1*. Under cell-free conditions, a decrease in absorbance measurement over time at 456 nm (Fig. 3) was also observed by spectrophotometry, confirming that BC is co-oxidized by *15-LOX-1*.

To determine if our Raman instrument is able to detect BC within a cellular system, we used ERC293 cells exposed to 0.3% MβCD alone or in combination with 0.2 or 1 μmol/L BC. After 24 hours of BC loading of ERC293 cells, we found that our Raman measurements of intracellular carotenoids correlated with the dose of BC/MβCD (see Table 1). These Raman measurements also correlated with the spectrophotometric measurements of BC after solubilization of the cells. The lack of linearity between our Raman and spectrophotometric measurements can be accounted for by a lack of absolute efficiency of BC extraction using our extraction method. However, these data suggest that BC loading of cells using MβCD is accurately detected by this Raman instrument.

We then tested whether our Raman instrument can detect a decrement in BC Raman signal after co-oxidation. Using our *15-LOX-1*–engineered ERC293 cells in the presence of BC, arachidonic acid, and ponasterone showed a significant decrement in Raman signal when compared with any component alone (Table 1). Additionally, HPLC confirmed a decrement of the parent BC peak area over time and identified the appearance of alternate peaks with shorter retention times, suggesting the appearance of BC oxidative metabolites (Fig. 4). Several interesting peaks showed retention times (t_R) and UV spectral λ_{max} characteristics similar to published BC breakdown products (ref. 23; Fig. 4C). These results suggest that oxidation can cause a breakdown of BC to shorter-chain, less polar molecular species that are less detectable by this resonance Raman instrument. These data show that our resonance-enhanced Raman instrument can detect the oxidative breakdown of BC in loaded cells as a decrease in BC Raman signal.

Use of the resonance-enhanced Raman instrument in patients

Using this fiberoptic prototype Raman instrument, a proof-of-concept pilot study was undertaken to measure concentrations in UADT tissues of 52 subjects (31 males; mean age, 47.3 ± 2.6 years; range, 19-83 years). Sixteen subjects within our study (30.8%) had head and neck squamous cell carcinoma (HNSCCa), whereas the rest (69.2%) were non–tumor-bearing controls. Eight subjects currently used tobacco, whereas another 18 admitted to former tobacco use, and the rest denied any prior tobacco intake. The mean pack-year smoking history (pack-years = number of packs per day × the number of years smoking in total) for smokers was 27.8 ± 33.5 pack-years. Twenty-two subjects admitted to active alcohol intake, five were former alcohol users, whereas the rest of the study cohort had never consumed alcohol. No significant differences were found between HNSCCa subjects and non–tumor-bearing controls with respect to tobacco or alcohol consumption ($P = 0.3$ and $P = 0.2$ by χ^2 test).

These investigations discovered some very provocative findings (Table 2). The test-retest reliability of our Raman instrument in these patients showed a relative SD of ±8%. Different subsites of the UADT showed significantly different Raman measurements ($P < 0.001$). Furthermore, subjects consuming or have consumed alcohol were found to have significantly higher Raman readings in certain UADT subsites when compared with non-drinking subjects ($P < 0.05$ for floor of mouth and soft palate). Interestingly, when controlling for age, sex, and tobacco use, lower Raman measurements were found in HNSCCa subjects ($P < 0.002$) compared with non–tumor-bearing subjects for the palate ($P = 0.002$) and approached significance for the floor of mouth ($P < 0.07$). These data show the feasibility of using this single-fiber resonance-enhanced Raman instrument and raise some potentially interesting points about carotenoid pharmacology and oxidative biology.

Discussion

These results show that our Raman prototype may provide significant advances in two disciplines of study: the fiberoptic probe design of this prototype adds the potential of clinical utility to the field of Raman spectroscopy, and this potentially clinically useful Raman instrument may help to define the tissue pharmacokinetics and oxidative biology of BC in live tissues.

Raman spectroscopy is a powerful technique able to use the unique vibrational and/or rotational energy of molecules to identify and quantify the concentration of molecules in biological samples. Carotenoids seem to be ideal as a molecule capable of evaluation in live tissues using this technology. These molecular species have particularly intense absorption bands in the blue/green wavelength range that result in one of the largest resonant enhancements ever encountered ($\approx 10^5$; ref. 19). No other biological molecules found in significant concentrations in human tissues exhibit similar resonant enhancement with blue laser excitation (488 nm) in this wave number region. Therefore, the *in vivo* carotenoid Raman spectra are remarkably free of confounding responses and can be used to analyze carotenoid concentrations within tissues under study.

Raman spectroscopy is increasingly being investigated as a noninvasive means to obtain an "optical biopsy" of human tissues under study. Examples of clinical use of Raman spectroscopy being actively investigated are areas such as the evaluation of potentially detrimental pathogens (29), tissue foreign body (30), dental disease (31), and cancers (32, 33). Clearly, the utility of Raman spectroscopy within human diseases has great potential, but certain obstacles must be overcome.

One obstacle to the full realization of clinical utility for Raman spectroscopy is the lack of a delivery system capable of accessing difficult anatomic sites (34). Investigative groups are exploring the use of a single fiberoptic mode of delivering and collecting Raman measurements (16–18), but systems that monitor a broad bandwidth are easily overwhelmed by background fluorescence obscuring relatively weak Raman signals. Our single-fiber resonance-enhanced Raman system able to provide both illumination and collection is made possible by the relative ease by which our software and optics can eliminate background fluorescence within a relatively narrow bandwidth of interest for carotenoids. This Raman instrument is potentially capable of determining relative concentrations of important antioxidant compounds, such as BC, in any endoscopically accessible live tissue with a high level of accuracy. Using this system, we have shown the ease of assessing relative concentrations of carotenoids in specific tissues at risk of tobacco-related cancer development and support future validation studies of this Raman prototype.

If our instrument is validated as a precise and accurate technology during future experimental efforts, these data raise some provocative possibilities about carotenoid oxidative metabolism. Given the results of the ATBC and CARET clinical trials in conjunction with the data presented herein, we hypothesize that carotenoids have a duality of function, being antioxidant under low oxidative stress conditions but becoming potent and long-acting pro-oxidants under a tobacco-induced highly oxidative environment. If found to be the case, the synergistic effects of alcohol consumption with tobacco in HNSCCa development may in part be explained by a concentration of carotenoids as a result of alcohol use within this tobacco-related oxidative environment. Oxidative breakdown of carotenoids could remove carotenoid-related species from the Raman measurable pool that our instrument detects, thus decreasing Raman signal. Moreover, these oxidative metabolites of carotenoids may potentiate cancer development through an enhancement of oxidative stress and/or influencing key cancer-related cellular pathways. If it is found that our Raman instrument is able to detect intact carotenoids but unable to detect its oxidative metabolites; Raman spectroscopy may become a very useful screening tool with which to measure unoxidized carotenoid concentrations in tissues at risk of cancer development during future carotenoid chemoprevention trials. These hypotheses are the focus of ongoing investigations.

In summary, we have engineered a single-fiber resonance-enhanced Raman spectroscope that is uniquely designed for clinical applications. In this study, we have shown that this Raman instrument can identify an increase in the concentrations of BC in cells and additionally denote the oxidative breakdown of BC after exposure to oxidative sources as a decrement in the Raman signal of the parent BC compound. Finally, these results provide proof of concept that this single-fiber instrument can potentially measure carotenoids in UADT tissues of patients or any other tissue accessible endoscopically. These data provide support for further validation of this technology as a precise and accurate technology for use during future carotenoid-based chemopreventive trials.

Disclosure of Potential Conflicts of Interest

No potential conflicts of interest were disclosed.

Acknowledgments

We would like to acknowledge Kenneth Boucher of Biostatistics for his statistical support in the preparation of the manuscript.

Grant Support

The Elsa U. Pardee Foundation and the American Academy of Otolaryngology-Head and Neck Surgery Foundation/American Head and Neck Society.

The costs of publication of this article were defrayed in part by the payment of page charges. This article must therefore be hereby marked *advertisement* in accordance with 18 U.S.C. Section 1734 solely to indicate this fact.

Received 07/29/2009; revised 09/09/2009; accepted 10/07/2009; published OnlineFirst 03/30/2010.

References

1. Mackay J, Jemal A, Lee NC, Parkin DM. The cancer atlas. Atlanta: American Cancer Society; 2006.
2. Mackay J, Eriksen M, Shafey O. The tobacco atlas. 2nd ed. Atlanta: American Cancer Society; 2006.
3. Jatoi I, Cummings KM, Cazap E. Global tobacco prolem getting worse, not better. J Onc Practice 2009;5:21–3.
4. Temple NJ. Re: "Dietary flavonoid intake and risk of cardiovascular disease in postmenopausal women". Am J Epidemiol 2000;151: 634–5.
5. Willett WC. Diet and health: what should we eat? Science 1994;264: 532–7.
6. Willett WC. Balancing life-style and genomics research for disease prevention. Science 2002;296:695–8.
7. Liu RH. Potential synergy of phytochemicals in cancer prevention: mechanism of action. J Nutr 2004;134:3479–85S.
8. Heber D, Lu QY. Overview of mechanisms of action of lycopene. Exp Biol Med (Maywood) 2002;227:920–3.
9. Greenberg ER, Baron JA, Stukel TA, et al, The Skin Cancer Prevention Study Group. A clinical trial of β carotene to prevent basal-cell and squamous-cell cancers of the skin. N Engl J Med 1990;323: 789–95.
10. The Alpha-Tocopherol, Beta Carotene Cancer Prevention Study Group. The effect of vitamin E and β carotene on the incidence of lung cancer and other cancers in male smokers. N Engl J Med 1994;330:1029–35.
11. Hennekens CH, Buring JE, Manson JE, et al. Lack of effect of long-term supplementation with β carotene on the incidence of malignant neoplasms and cardiovascular disease. N Engl J Med 1996;334: 1145–9.
12. Omenn GS, Goodman GE, Thornquist MD, et al. Effects of a combination of β carotene and vitamin A on lung cancer and cardiovascular disease. N Engl J Med 1996;334:1150–5.
13. Faulks RM, Southon S. Challenges to understanding and measuring carotenoid bioavailability. Biochim Biophys Acta 2005;1740:95–100.
14. Bernstein PS, Yoshida MD, Katz NB, McClane RW, Gellermann W. Raman detection of macular carotenoid pigments in intact human retina. Invest Ophthalmol Vis Sci 1998;39:2003–11.
15. Hata TR, Scholz TA, Ermakov IV, et al. Non-invasive Raman spectroscopic detection of carotenoids in human skin. J Invest Dermatol 2000;115:441–8.
16. Koljenovic S, Bakker Schut TC, Wolthuis R, et al. Tissue characterization using high wave number Raman spectroscopy. J Biomed Opt 2005;10:031116.
17. Koljenovic S, Schut TC, Wolthuis R, et al. Raman spectroscopic characterization of porcine brain tissue using a single fiber-optic probe. Anal Chem 2007;79:557–64.
18. Santos LF, Wolthuis R, Koljenovic S, Almeida RM, Puppels GJ. Fiber-optic probes for *in vivo* Raman spectroscopy in the high-wavenumber region. Anal Chem 2005;77:6747–52.
19. Bernstein PS, Zhao DY, Sharifzadeh M, Ermakov IV, Gellermann W. Resonance Raman measurement of macular carotenoids in the living human eye. Arch Biochem Biophys 2004;430:163–9.
20. Bernstein PS, Zhao DY, Wintch SW, Ermakov IV, McClane RW, Gellermann W. Resonance Raman measurement of macular carotenoids in normal subjects and in age-related macular degeneration patients. Ophthalmology 2002;109:1780–7.
21. Ermakov IV, Ermakova MR, McClane RW, Gellermann W. Resonance Raman detection of carotenoid antioxidants in living human tissues. Opt Lett 2001;26:1179–81.
22. Gellermann W, Ermakov IV, Ermakova MR, McClane RW, Zhao DY, Bernstein PS. *In vivo* resonant Raman measurement of macular carotenoid pigments in the young and the aging human retina. J Opt Soc Am A Opt Image Sci Vis 2002;19:1172–86.
23. Wu Z, Robinson DS, Hughes RK, Casey R, Hardy D, West SI. Co-oxidation of β-carotene catalyzed by soybean and recombinant pea lipoxygenases. J Agric Food Chem 1999;47:4899–906.
24. Cordray P, Doyle K, Edes K, Moos PJ, Fitzpatrick FA. Oxidation of 2-cys-peroxiredoxins by arachidonic acid peroxide metabolites of lipoxygenases and cyclooxygenase-2. J Biol Chem 2007;282: 32623–9.
25. Yu MK, Moos PJ, Cassidy P, Wade M, Fitzpatrick FA. Conditional expression of 15-lipoxygenase-1 inhibits the selenoenzyme thioredoxin reductase: modulation of selenoproteins by lipoxygenase enzymes. J Biol Chem 2004;279:28028–35.
26. Pfitzner I, Francz PI, Biesalski HK. Carotenoid: methyl-β-cyclodextrin formulations: an improved method for supplementation of cultured cells. Biochim Biophys Acta 2000;1474:163–8.
27. Chichili GR, Nohr D, Frank J, et al. Protective effects of tomato extract with elevated β-carotene levels on oxidative stress in ARPE-19 cells. Br J Nutr 2006;96:643–9.
28. WHO Brief Intervention Study Group. A cross-national trial of brief interventions with heavy drinkers. Am J Public Health 1996;86: 948–55.
29. Kalasinsky KS, Hadfield T, Shea AA, et al. Raman chemical imaging spectroscopy reagentless detection and identification of pathogens: signature development and evaluation. Anal Chem 2007;79: 2658–73.
30. Schaeberle MD, Kalasinsky VF, Luke JL, Lewis EN, Levin IW, Treado PJ. Raman chemical imaging: histopathology of inclusions in human breast tissue. Anal Chem 1996;68:1829–33.
31. Sowa MG, Popescu DP, Werner J, et al. Precision of Raman depolarization and optical attenuation measurements of sound tooth enamel. Anal Bioanal Chem 2007;387:1613–9.
32. Frank CJ, McCreery RL, Redd DC. Raman spectroscopy of normal and diseased human breast tissues. Anal Chem 1995;67:777–83.
33. Koljenovic S, Schut TB, Vincent A, Kros JM, Puppels GJ. Detection of meningioma in dura mater by Raman spectroscopy. Anal Chem 2005;77:7958–65.
34. Griffiths J. Raman spectroscopy for medical diagnosis. Anal Chem 2007;79:3975–8.